

**SITE DIRECTED MUTAGENESIS IN THE
P-SPECIFIC CONSERVED REGION OF
HISTONE NUCLEAR FACTOR-P**

A Major Qualifying Project Report

Submitted to the Faculty of the

WORCESTER POLYTECHNIC INSTITUTE

in partial fulfillment of the requirements for the

Degree of Bachelor of Science

in

Biology and Biotechnology

by

Timothy F. Buck

January 10, 2007

APPROVED:

Janet L. Stein, Ph.D.
Cell Biology Dept.
UMass. Medical Center
Major Advisor

David Adams, Ph.D.
Biology and Biotechnology
WPI Project Advisor

Abstract

Histone Nuclear Factor-P (HiNF-P) is the final link in a CyclinE/CDK2à p220^{NPAT} pathway to cell cycle-dependent transcription of histone H4. In this project, mutations were introduced to HiNF-P to study the biological effects of the P-Specific Conserved Region (PSCR), a highly conserved region whose specific activity is unknown. Assays were carried out to quantify expression (Western), subcellular localization (immunofluorescence), DNA binding (EMSA), and H4 promoter activity (luciferase). The data strongly suggest that the first twenty amino acids of the PSCR are essential for DNA binding.

Table of Contents

Abstract	2
Table of Contents	3
Acknowledgments	4
Background	6
Project Purpose	17
Materials and Methods	20
Results	26
Discussion	40
References	46

Acknowledgments

It is by no accident that I started and finished this project successfully. I am forever grateful for my acceptance into one of the most enjoyable work environments I could ever have imagined. Many people have helped me to initiate, execute, and analyze the enormous amounts of data I've acquired, and I thank each and every one of you.

First and foremost, I wish to thank my four principal investigators; Janet Stein, Gary Stein, Andre van Wijnen, and Jane Lian, for allowing me to start my work on HiNF-P nearly two years ago. Thank you especially to Janet Stein for editing my draft while reviewing other articles, and reports. The four of you provided me with a dream summer job that turned into a fascinating research project. You have always provided me with answers to my toughest questions, and given constructive criticism even at the most difficult times. I would also like to thank my WPI academic advisor, Dave Adams, for helping me plan out my time at WPI, helping me to initiate this project, and continuing to teach the most intellectually stimulating classes at WPI.

There were many students and post docs in the lab who shared their specialty with me in order to complete my project. For your vast assistance in helping me with immunofluorescence, offering new and stimulating ideas, and a constant level of sarcastic humor, thank you very much, Kaleem Zaidi. For helping me get on my feet my first few months in the lab thank you to Jitesh Pratap, and Angela Miele. For assistance in the Luciferase assay conditions, thank you, Margaretha van der Deen.

Thank you to my entire lab for all the encouragement, scientific discussions, birthday celebrations, sharing of buffers and instruments, and always asking, “Tim, lunch?”

Lastly I never would have gone anywhere with HiNF-P if it was not for Ricardo Medina. Thank you, Ric, for being my mentor for these past two years. Thank you for finishing up the last step in an experiment when I had to run back to WPI; Thank you for splitting my cells on Saturday so that they would be ready for me on Monday, and for initially agreeing to work with me. The scientist inside me owes you a great deal for sharing your knowledge, experience, and, of course, your impeccable organizational skills with me.

Background

For decades an understanding of the process by which cells divide and proliferate has been highly sought after but even with decades of research, still much is not understood. Eukaryotic cells go through a highly regulated cell cycle in order to divide. This process consists of four steps: G₁, S (synthesis), G₂, and M (mitosis), each describing key events of the cell during this time period (Figure 1). There are also checkpoints at the end of each stage that make sure the cell does not progress to the next stage until it is ready to do so (Alberts et al., 2002). Of particular interest is the junction where the cell moves from a state of development in preparation for division, G₁, to the synthesis of new DNA, S phase. This point, known as the G₁/S transition, is where replication-dependent histones are produced.

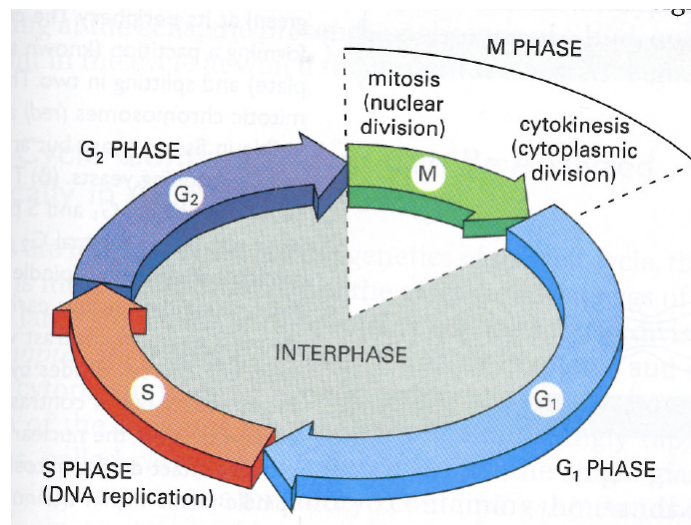


Figure 1. The Eukaryotic Cell Cycle (Alberts et al., 2002).

Histones and DNA Packaging

Histones have a very special task to package up the lengthy DNA into small compact nucleosomes. Their impressive ability to accomplish this is highlighted by the fact that histones effect an approximate compression ratio of 1000-fold on the DNA (Alberts *et al.*, 2002). The five histones H1, H2A, H2B, H3, and H4 all take part in creating the nucleosome. Two molecules of H2A, H2B, H3, and H4 form the histone octamer, around which the double stranded DNA is wound. These histones are also referred to as the core histone proteins. To form the histone octamer, H3 and H4, along with H2A and H2B form dimers with each other. The H3 - H4 dimers form a tetramer, and the two H2A-H2B dimers form around the tetramer completing the histone octamer. Once the DNA is wound around the octamer, a final histone H1 is added to the nucleosome, binding the histone core proteins and DNA, helping to compact the structure (Alberts *et al.*, 2002). Figure 2 shows this chromatin packaging process, which eventually ends with the final compact genetic infrastructure, the chromosome.

Control of Histone Synthesis

Not only are the histone proteins themselves vital, but the multiple synchronized processes that regulate histone synthesis are of the utmost importance, as it has been shown that unbalanced levels of histone proteins can cause loss of chromosomes (Meeks-Wagner & Hartwell, 1986). Histones have a very specific and important function, which is needed when new DNA is being synthesized. Though variants of histones are produced at basal levels throughout the cell cycle, 90% are replication-dependent and transcribed during S phase. The production of histone mRNA is controlled by three pathways (Wu

and Bonner, 1981). The first level of histone transcriptional control is at the G1/S transition. Here, histone mRNA synthesis is increased three to five fold over the preceding G1 stage (Reviewed in Osley, 1991). The remaining five to six fold additional histone mRNA increase is accounted for at the posttranscriptional level.

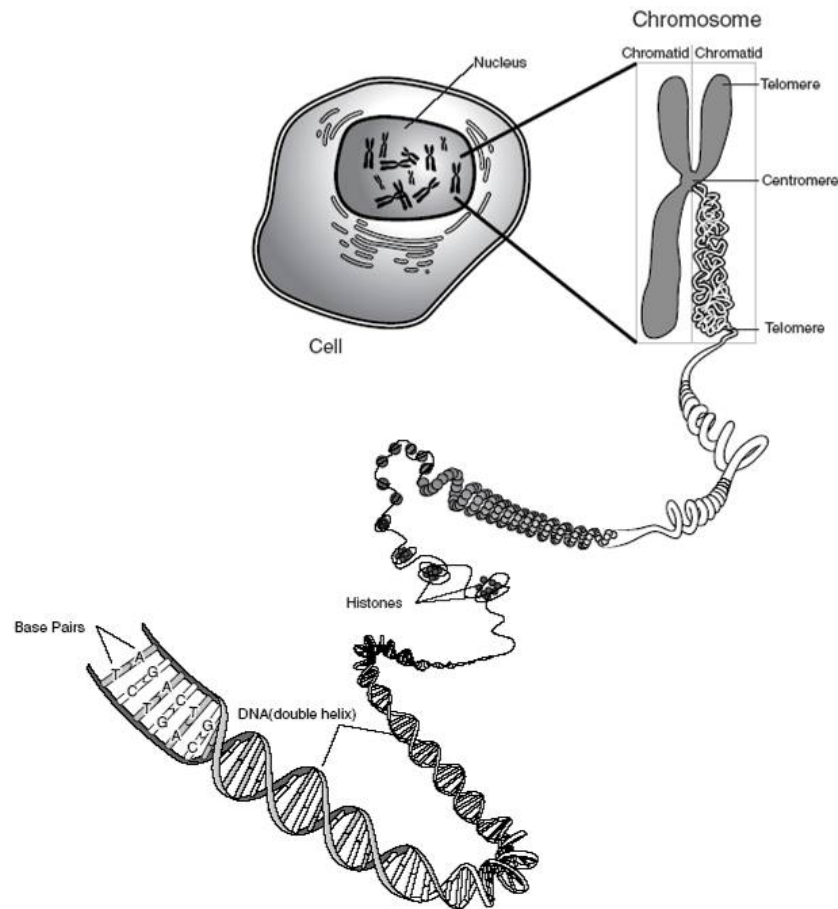


Figure 2. Structural Overview of the Genome. Double stranded DNA is wound around the histone core proteins to create the nucleosome. Multiple nucleosomes are further compacted into chromatin, which makes up the chromosome. (National Institutes of Health)

The first posttranscriptional pathway causes an increase in the histone mRNA half life. The half life of histone mRNA when chromosome replication is blocked has been experimentally estimated to be between 10 to 15 minutes. During S phase, however, the histone mRNA half life increases to 30 to 60 minutes (Reviewed in Osley, 1991). This enables the already increasing amounts of histone mRNA to last for a longer duration.

The second posttranscriptional pathway deals with the processing of histone pre-mRNAs. Before histones can become mature and functional cytoplasmic mRNAs, their 3' ends must be processed by endonucleases. Harris *et al.* (1991) showed that increased 3' processing leads to a six to eight fold increase in histone mRNA levels (Reviewed in Osley, 1991). These three regulatory mechanisms account for the large induction of histones at a crucial time when these specific proteins are needed the most.

Histone H4/n Gene as a Model for Histone Behavior

In order to study the effects of HiNF-P on histone function, the selection of a model gene and analogous protein was necessary. Because histone H4 is the most highly conserved protein in the nucleus, it was the ideal candidate to select as a model histone. The corresponding mRNA transcript was also well characterized making it appropriate to study cell cycle related effects (Mitra *et al.*, 2003; Braastad *et al.*, 2004). To ensure consistency in experimental results, the H4/n subtype was selected as the model gene, which which HiNF-P would be tested. Though the amino acid sequences of all histones are highly conserved because of the essential role histones play in DNA packaging, H4 is *the* most conserved compared with all histone proteins (Alberts *et al.*, 2002; Mitra *et al.*, 2003).

Site II (Figure 3) plays an important role in the histone H4/n gene. The histone H4/n gene contains two protein binding sites within the proximal promoter; Site I is located from nt -150 to -113, and Site II located from nt -97 to -47 (Pauli, *et al.*, 1987; Van Wijnen, *et al.*, 1992). Site II contains a highly conserved nucleotide sequence unique to the many of H4 genes located in the human genome. This sequence contains

many G residues necessary for DNA-protein interactions (Mitra *et al.*, 2003). Studies have shown that there are several histone nuclear binding factors (HiNFs) that have the ability to bind to Site II, named HiNF-D, HiNF-M, and HiNF-P (van Wijnen *et al.*, 1991).

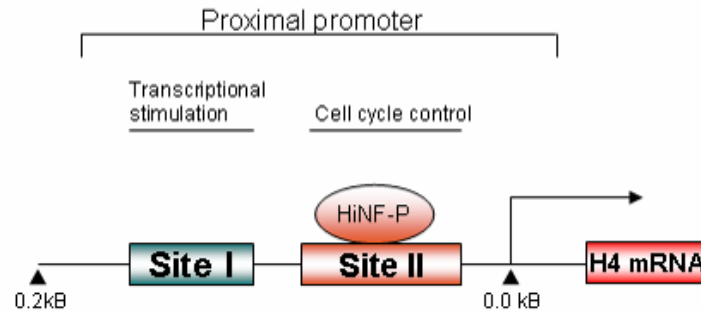


Figure 3. HiNF-P binds to Site II of the H4/n Proximal Promoter. While there are other proteins that interact with Site I and Site II this figure only shows HiNF-P for clarity. Adapted from van Wijnen *et al.* (1992).

Activation of Histone H4/n via the Cyclin-E Pathway

The signaling pathway that allows cells to progress into the S phase is ultimately linked to the cell's ability to synthesize functional histones. When cells are ready to begin proliferation, they initiate a signal cascade beginning with growth factors which activates a master transcription factor E2F. E2F is one of the most highly studied transcription factors because it has such a global effect on how cells progress through the cell cycle. It is responsible for the transcription of many proteins required for progression into S phase (Stevens and Thangue, 2003). Even though E2F is known to activate G1/S specific genes, it can not directly activate histone H4/n because the cell cycle regulatory site II lacks well known and widely accepted E2F binding sites (van Wijnen *et al.*, 1991 and Stevens and

Thangue). This means E2F must initiate a signal cascade in which other downstream messengers activate histone transcription (Figure-4). These downstream messengers have been characterized by many researchers, and are described in detail below.

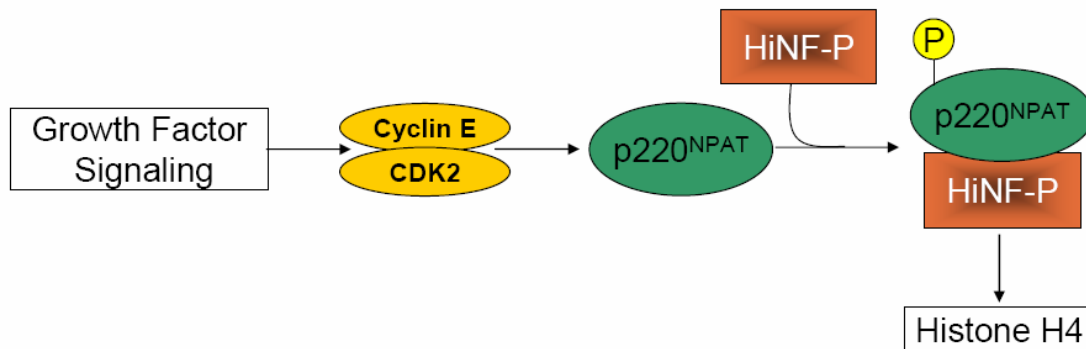


Figure 4. Overview of the Cyclin E/CDK2/p220^{NPAT}/ HiNF-P Pathway for Activating Histone H4.
Adapted from Stein *et al.* (2006).

Cyclin E

One of the initial downstream targets of E2F is cyclin E. Cyclin E is sometimes referred to as the “master cyclin” because it is able to overcome deficiencies in other G1/S specific cyclins. Cyclin E also shows increased expression at the G1/S boundary. This increased expression is due in part to Cyclin E’s ability to stimulate the transcription of additional cyclin E by disassociating from repression caused by p27^{Kip1}. Cyclin E’s elevated expression coincides at a point where it is needed the most to promote S phase entry, and activate CDK2 (Möröy & Geisen, 2004).

CDK2

Cyclin dependent kinases (CDK) are a group of cell cycle related enzymes which are inactive until they are bound with their appropriate cyclin (Möröy & Geisen, 2004). When the appropriate cyclin protein binds the CDK, the CDK active site is exposed allowing phosphorylation of specific downstream targets. In the case of histone gene regulation, the complex is comprised of cyclin E and its partner CDK2. Looking further downstream in the pathway, the cyclin E/CDK2 complex plays a role in histone regulation by phosphorylating and activating p220^{NPAT}, the next messenger in the process (as shown in green in Figure 4).

p220^{NPAT}

The identification of p220^{NPAT} in 1996 represented a relatively new gene in cell cycle related research (Imai *et al.*, 1996). With the identification of p220^{NPAT} researchers discovered that it binds to and is phosphorylated by the cyclin E/CDK2 complex (Zhao *et al.*, 1998; Ma *et al.*, 2000). Though this establishes its upstream links, the connection of p220^{NPAT} and histone gene regulation was made by observing that p220^{NPAT} localizes to Cajal bodies, small nuclear organelles hypothesized to be the site where transcription and splicing complexes are assembled (Gall *et al.*, 1999). NPAT's Cajal localization creates links to histone regulation because some Cajal bodies are physically linked to histone gene clusters. Cajal bodies are also involved in the 3' processing which histone mRNAs must go through to be active (Frey & Matera, 1995; Abbott *et al.*, 1999). These observations, the physical link and 3' processing, strongly suggest that p220^{NPAT} is involved in cell cycle-dependent histone regulation.

The relationship between HiNF-P and p220^{NPAT} has only just begun to unfold. *In vitro* synthesized HiNF-P and p220^{NPAT} co-immunoprecipitations show that detection of HiNF-P when precipitating p220^{NPAT} (and *vice versa*) is easily achievable, proving a physical interaction of HiNF-P and p220^{NPAT}. To define the p220^{NPAT} interaction region, deletion mutants of p220^{NPAT} were created and show that three regions are necessary for interaction with HiNF-P. These regions of p220^{NPAT} are from amino acids 1-46, 121-145, and 208-318 (Miele *et al.*, 2005). In addition, the relationship of HiNF-P and p220^{NPAT} in a functional manner was investigated. Luciferase reporter constructs that had the HiNF-P H4 promoter binding site mutated were created, and this experiment showed a decrease in p220^{NPAT} driven luciferase activity (Zhao *et al.* 2000). This data suggest a physical interaction between HiNF-p and p220^{NPAT}.

To support these p220^{NPAT} observations that p220^{NPAT} is involved in cell cycle-dependent histone regulation, Zhao *et al* (1998) demonstrated that (1) p220^{NPAT} directly associates with histone gene clusters; and (2) that histone H2B and H4 transcription increases by overexpressing p220^{NPAT}. Ma *et al.* (1998) established (3) that p220^{NPAT} is phosphorylated on CDK2 sites, and cyclin E is located at these foci; Lastly (4) mutating the CDK2 phosphorylation sites on p220^{NPAT} causes a reduction in H2B reporter gene expression. These results support the preliminary observations that p220^{NPAT} is linked to histone gene regulation, but it is not the final regulatory step.

HiNF-P

HiNF-P (orange box in Figure-4) is the final step in the cyclin E/CDK2/p220^{NPAT} pathway regulating cell cycle dependent histone gene transcription. p220^{NPAT} requires

another messenger to enable histone transcription because it does not contain any known DNA binding motifs (Miele *et al.*, 2005). HiNF-P has been identified as a protein able to bind to the histone H4 gene promoter, and is necessary for histone H4 transcription (Mitra *et al.*, 2003). Because HiNF-P is associated with the H4 promoter, it is likely able to recruit p220^{NPAT}. Miele *et al.* (2005) demonstrate that p220^{NPAT} requires HiNF-P to activate H4 by showing a decrease in p220^{NPAT} dependent H4 promoter activity when HiNF-P is silenced by RNAi. This experiment proves that HiNF-P is the final link in the signal cascade.

HiNF-P is part of a family of histone nuclear binding factors (HiNFs), which have been shown to bind to the H4 site II transcriptional regulatory element (Figure 3) (van Wijnen *et al.*, 1991). Full length HiNF-P has a molecular weight of 65 kDa, and consists of 517 amino acids. Figure 5 shows that HiNF-P contains 9 zinc fingers which are characteristic of one type of a DNA binding protein (Alberts *et al.*, 2002; Mitra *et al.*, 2003). Database analysis revealed that HiNF-P is identical to MIZF, a protein identified to interact with MBD2, a methyl-CpG-binding protein (Mitra *et al.*, 2003). Figure 5 also highlights in blue the HiNF-P specific conserved region (PSCR). This region near the C-terminus of HiNF-P is highly conserved throughout many species (Figure 6), thus this evolutionarily conserved region likely plays an important role in HiNF-P function (Mitra *et al.*, 2003).



Figure 5. HiNF-P Protein Schematic. HiNF-P is a 517 amino acid protein and consists of nine zinc fingers (yellow), two acidic regions (green) and the PSCR (blue).

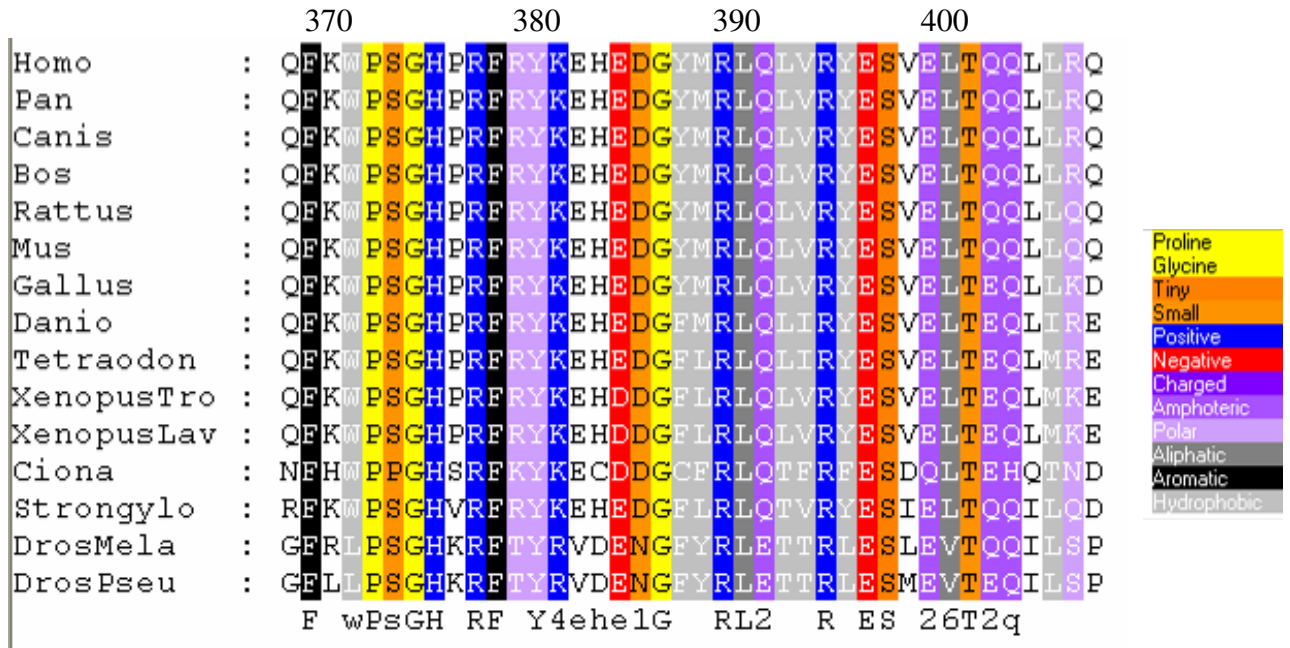


Figure 6. Amino Acid Alignment of the HiNF-P Specific Conserved Region (PSCR). The PSCR, from aa S374 to R407, is highly conserved throughout many organisms.

HiNF-P is also a proven activator of histone H4. Research has shown that overexpression of HiNF-P results in three fold enhancement of H4 promoter activity. The same result is not observed when the binding site on the promoter is mutated. In an artificial construct with three copies of the HiNF-P binding site fused to a TATA box, a six to seven fold activation of H4 promoter activity was observed. As a control to show HiNF-P specific activation, the large induction was not observed when the three binding sites were mutated so that HiNF-P could not bind (Mitra *et al.*, 2003).

Over all, HiNF-P is required for efficient S phase progression. The G1/S check point requires the presence of HiNF-P in order to move into S phase efficiently. HiNF-P deficient cells were generated, and their cell cycle progression was studied. It was shown that HiNF-P-deficient cells do not cause a complete cell cycle block, but slow the cell cycle progression into S phase. Even though HiNF-P expression levels were decreased in the cells, other compensatory transcription factors were likely present and carry on at

diminished levels (Mitra *et al.*, 2003). These data show a direct link between the presence of HiNF-P and the progression through the cell cycle.

Project Purpose

Previous research revealed that protein HiNF-P is responsive to the Cyclin E/CDK2/p220^{NPAT} pathway, is the final link in replication dependent histone H4 regulation, and is crucial for effective cell entry into S phase (Mitra *et al.*, 2003; Miele *et al.*, 2005). In this report we wanted to closely examine what roles the HiNF-P specific conserved region (PSCR) plays in histone H4/n gene transcription. This 34 amino acid region (See Figure 6 from aa S374 to R407) is an area of high amino acid sequence homology, but its function is still unknown. We created 23 point and deletion mutants within or shortly following PSCR. A deletion mutant encompassing the entire PSCR was also generated (See Figures 7 and 8 below). By creating HiNF-P mutants with specific amino acids that were replaced, or that lacked specific portions, we were able to correlate changes in H4/n transcriptional activity with the location of the mutation.

All point mutations were changed to alanine residues, except one which was mutated to phenylalanine preserving the aromatic structure of the original amino acid. Both alanine and phenylalanine prevent any interactions that the original amino acid could have participated in. Deletion mutations were selected because they systematically identified what spans of HiNF-P and the PSCR were involved in histone H4 regulation. Double mutations were also analyzed with both amino acids changed to alanine.

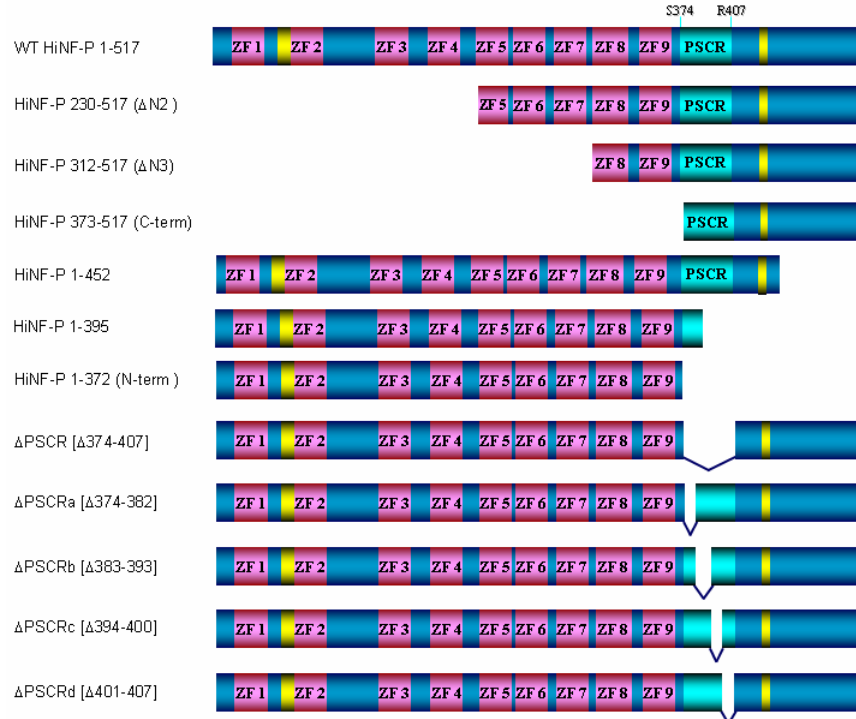


Figure 7. Deletion mutants in HiNF-P.

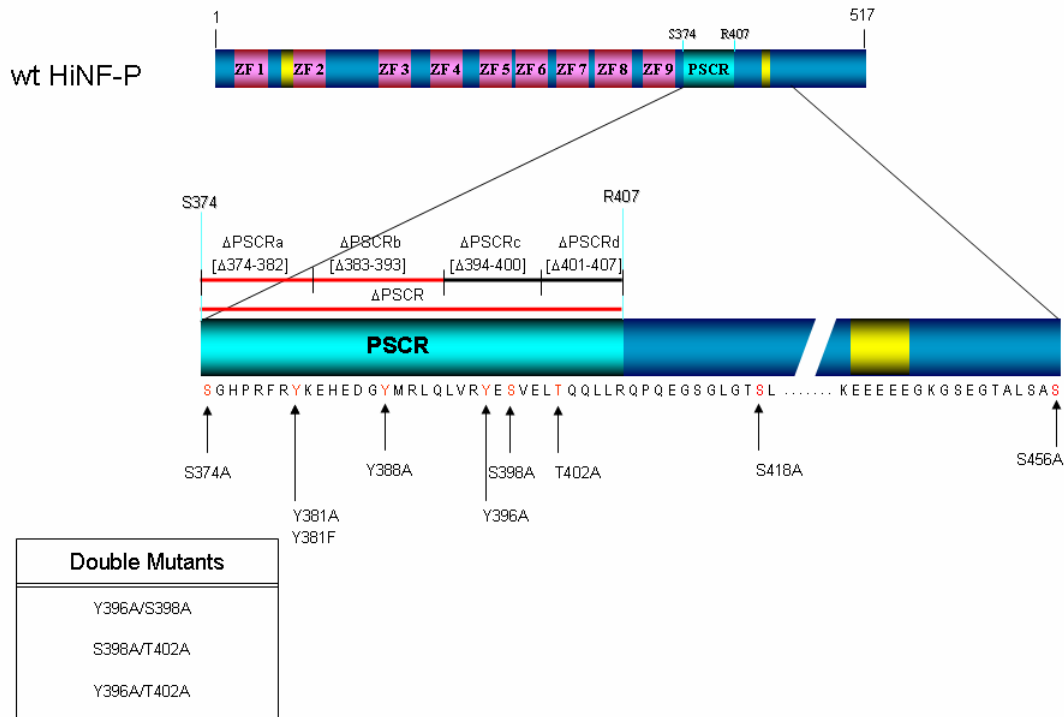


Figure 8. Point and double mutations in HiNF-P.

To answer our question we needed to observe both DNA binding activity and functional interactions of HiNF-P with H4/n. We tested the HiNF-P mutants, to see if the mutations were able to bind the histone H4/n promoter (DNA binding activity) and to see if the mutations had an effect on the H4/n promoter (functional), using *in vitro* and *in vivo* approaches. The results identify the first twenty amino acids of the PSCR as a region that is highly likely to be important for HiNF-P DNA binding activity.

Materials and Methods

Mutagenesis. Mutant oligonucleotides were designed following the instructions provided by Stratagene's QuickChange® Site-Directed Mutagenesis Kit (cat. 200518).

Oligonucleotides were obtained commercially or synthesized in house using a Beckman Oligo 1000M DNA synthesizer. All oligonucleotides were gel purified by denaturing polyacrylamide gel electrophoresis. Reactions were carried out following the manufacturer's instructions using pFLAG-HiNF-P as a template. Two clones of each mutant construct were selected. All final HiNF-P mutant constructs were confirmed by full length sequencing. The oligonucleotides used to generate the mutants are listed in the table below.

Name	5' Sequence 3'
S374A	CAAGTGGCCCGCAGGGCATCCCC
ΔPSCR	GTTCAAGTGGCC CC AACCACAAGAGG
ΔPSCRa	GTTCAAGTGGCC CG AACATGAAGATGGC
ΔPSCRb	CCCGTTTT CG GTACAAGGTTTCGCTACG
ΔPSCRc	GCTGCAGCT GC TGACACAGCAACTG
ΔPSCRd	CTACGAGAGTGTAGAG GC AACCACAAGAGG
Y381F	CATCCCCGTTTTTCGGT <u>TC</u> CAAGGAACATGAAGATGG
Y381A	GGCATCCCCGTTTTTCGGG <u>CA</u> AAGGAACATGAAGATGGCT
Y388A	AAGGAACATGAAGATGGCG <u>CA</u> ATGCGGCTGCAGCTGG
Y396A	CTGCAGCTGGTTCGCGCAGAGAGTGTAGAGCTGAC
S398A	GCTGGTTCGCTACGAGG <u>CAG</u> TAGAGCTGACACAGC
T402A	CGAGAGTGTAGAGCTGGC <u>CA</u> CAGCAACTGC
S418A	GGCCTGGGAACGGCCCTGAACGAGAGC
S456A	CCCTCTCAGCCGCTCAGGACAACCC
Y396A/S398A*	CAGCTGGTTCGCGCCGAGG <u>CAG</u> TAGAGC
T402A/Y396A**	GAGTGTAGAGCTGGCAGCAACTGCTGCGG
T402A/Y398A***	<u>GGCAG</u> TAGAGCTGGCAGCAACTGCTG

Table 1. Mutant oligonucleotides used to create HiNF-P mutants. The underlines indicate what nucleotides were changed, bold font indicates where the deletion is located. * Backbone template was pFLAG-S398A-HiNF-P, ** Backbone template was pFLAG-S396A-HiNF-P. ***Backbone template was pFLAG-Y398A-HiNF-P

Transient Transfections. Cells were seeded so on the day of transfection they were 40-50% confluent. Twenty-four hours later, cells were washed with room temperature PBS, and complete media warmed to 37°C was added. Transfection was achieved using a ratio of 1 µg of DNA: 3 µl of transfection reagent FuGENE6 (Roche) in incomplete media. The DNA/FuGENE6/media mix was vortexed gently and allowed to incubate for 15 minutes at room temperature. The mixture was added drop-wise to the cells. Plates were gently swirled afterwards.

Nuclear Extract Preparation. HeLa cells were seeded at 0.5×10^6 and twenty-four hours later transfected with the indicated plasmids (4 ug per 100 mm plates of each construct; see above for transfection methods using FuGENE6). Twenty-four hours after transfection, cells were washed with ice cold PBS and transferred to a tube where they were centrifuged at 1,000g for 5 minutes at 4 °C in an Eppendorf Centrifuge 5415R. All subsequent procedures were done at 4°C, and centrifuged in the Eppendorf Centrifuge 5415R . The supernatant was carefully aspirated, and the pellet was suspended in cold NP-40 lysis buffer (10mM Tris-HCl (pH 7.4), 3mM MgCl₂, 10mM NaCl, 0.5% NP-40) by pipetting gently up and down until the mixture was homogenous. The sample was left on ice to incubate for 10 minutes, and then spun at full speed for 30 seconds. The supernatant was removed, and the pellet was re-suspended by pipetting in 400ul of cold Hypotonic Buffer (10mM Hepes (pH 7.9), 1.5 mM MgCl₂, 10 mM KCl). Samples were spun in the same centrifuge at 4,500g for 1 minute, supernatant removed, and 100 ul of cold Extraction buffer (20 mM Hepes (pH 7.9), 1.5 mM MgCl₂, 420 mM KCl, 0.2mM

EDTA, 20% glycerol) was added. Samples were left to rock in cold room for 45 minutes. After rocking, samples were spun at full speed for 5 minutes, the supernatant containing the nuclear extracts was harvested and quickly frozen in liquid nitrogen and kept at -80° C until use.

In vitro transcription and translation. Proteins were synthesized using Promega's TNT T3 Quick Coupled Transcription/Translation System (cat. L1170), following the provided protocol. The integrity of IVTT produced proteins was checked by western blots.

Immunofluorescence microscopy. All procedures were done at 4°C, unless otherwise noted. SaOS cells were plated at 0.08×10^6 cells per well in a six-well plate (Corning), onto dried coverslips coated in 0.5% Difco™ Gelatin (BD Sciences). Cells were taken 24 hours after transfection with 0.5 ug of each construct (as described above) on ice and washed twice with ice cold PBS. Whole cell fixative (2 mL; 3.7% formaldehyde in PBS) was added to each well, for 10 minutes. Wells were aspirated, and washed once with ice cold PBS. Permeabilizing solution (1 mL; 0.25% Triton X-100 in PBS) was added to each well for 20 minutes. Wells were aspirated, and 1 mL of PBSA (0.5% Bovine serum albumin in PBS) was added to each well. The lids of each six well plate were covered with Parafilm, and a drop of the primary antibody (20 ul; Sigma M2 Mouse α FLAG 1:4,000 in PBSA) was added on the Parafilm. Coverslips were placed cell side down on the antibody drop, and incubated at 37 °C in the dark for 1 hour. Coverslips were placed back in their respective wells facing upwards, and washed four times with ice cold PBSA.

Secondary antibody (20 μ l; Alexa 488 Goat α Mouse 1:800 in PBSA) was added to a new strip of Parafilm in the exact same way as primary, and incubated at 37 °C in the dark for 1 hour. Coverslips were placed back in their respective wells facing upwards, and washed four times with ice cold PBSA. Cells were DAPI stained (0.5 μ g/mL DAPI in 0.1% TritonX 100-PBS) for 5 minutes on ice. Cells were washed once in 0.1% TritonX-100/PBS, then twice with ice cold PBS. Coverslips were immediately mounted using ProLong Gold antifade reagent (Invitrogen), and sealed. Slides were stored at -20°C.

Western Blots. Samples were prepared by mixing with gel loading buffer (final concentration 50 mM Tris-Cl pH6.8, 100 mM DTT, 2% SDS, 0.2% Bromophenol blue, and 10% glycerol), and boiling for 5 minutes. Prepared samples and molecular weight marker (Bio-Rad cat. 161-0374) were electrophoresed on an SDS-10% or 4-15% gradient gel (Bio-Rad) and blotted onto a polyvinylidene difluoride Immobilon-P membrane (Millipore). Immunodetection was performed using primary antibodies directed against mouse monoclonal or rabbit polyclonal FLAG (1:4,000 to 1:8,000), mouse monoclonal FLAG-HRP (1:5,000), or rabbit polyclonal HiNF-P (1:5,000). Western Lightning Chemiluminescence Reagent Plus (Perkin Elmer Life Sciences) was used to detect the signal.

Electrophoretic Mobility Shift Assays (EMSAs) were performed incubating the probe (20 fmol of labeled site II H4/n probe with at least 20,000cpm), and a constant total amount of protein (IVTT: 1-2 μ l; NuE: 2-5 μ g) in Buffer C (50 mM KCl, 10% glycerol

0.1 ug/ul salmon sperm DNA used as a non specific competitor, 1 mM DTT, 0.5 mM MgCl₂, and 0.1 mM ZnCl₂) for twenty minutes at room temperature. All competitors (See Table 2 for sequence) were added in 100X molar excess, for reactions with no competitors water was added to keep the total volume the same. Samples were run on a non denaturing polyacrylamide gel, and when finished they were vacuum dried at 80°C to filter paper, and exposed to a Kodak BioMax XAR or MR X-ray film. Film was exposed to the gels at -80°C for varying lengths, allowed to warm to room temperature, and then developed.

Competitor	5'- Sequence- 3'
Specific	CTTCAGGTTTTCAATCTGGTCCGATACT
HiNF-P mutant	CT CAGGTTTTCAATCTTCT <u>AC</u> GATACT
Non specific SP1	ATTCGATCGGGGCGGGGCGAGC

Table 2. EMSA competitor sequences. Specific competitor sequence was derived from the Site II HiNF-P binding site. Underlines indicate deviation from consensus sequence.

Luciferase Assay. Luciferase assays were carried out using Promega's Dual-Luciferase[®] Reporter Assay System (cat. E1960). U2-OS cells were seeded at 0.13 x 10⁶ cells per well in six-well plates. 24 hours later cells were washed with room temperature PBS, and 2 mL/well complete McCoy's media warmed to 37°C was added. DNAs used per well were: 200 ng of the reporter p3x site II/Luc construct, 5 ng of phRL-null (Promega) to normalize for transfection efficiency, 200 ng of p220^{NPAT} and variable amounts of wild type or mutant HiNF-P. After 24 hours, transfected U2-OS cells (see transfection methods above) were incubated with 250 ul/well of 1x Passive Lysis Buffer for 15 minutes at room temperature. Plates were gently swirled during the incubation on an orbital shaker. After incubation, 20 ul of each well was sampled in a 96-well COSTAR Assay Plate and the relative light unit was determined using the Dual Luciferase Reporter Assay System

in a Glomax luminometer (Promega). Firefly luciferase values were normalized to *Renilla* luciferase, and then values adjusted with the empty vector being equal to 1. Lysate samples were prepared for western blot by spinning samples for 5 minutes at full speed at 4 °C, and mixing 12 ul with 6 ul of 3X PAGE gel loading buffer (as described above).

Results

To ensure that mutations introduced into HiNF-P did not have an effect on the subcellular localization, SaOS cells were transfected with WT or mutant HiNF-P, and harvested for whole cell immunofluorescence microscopy. In Figure 9 images are presented showing that wild type and all types of mutant HiNF-P (green) are localized exclusively in the nucleus (blue). The phase image shows that the cell has the correct morphology and is a healthy cell. Two mutants displayed slightly higher HiNF-P staining in the cytoplasm (HiNF-P 312-517 (Δ N3), and HiNF-P mutant S398A), but the majority of the staining was nuclear. It is possible that this small cytoplasmic expression was caused by the over-expression of mutant HiNF-P. Though only one image is displayed for each mutant, the image selected is a representative photograph of all the cells viewed on the slide.

Previous studies have used Electrophoretic Mobility Shift Assays (EMSAs) to check the ability of the HiNF-P to bind DNA (van Wijnen, *et al.*, 1992; Mitra *et al.* 2003). These highly sensitive assays allow quantification of binding ability, relative to wild type binding activity. We analyzed the DNA binding activity of HiNF-P mutants with a histone H4/n DNA probe, using both HiNF-P from Nuclear Extracts (NuE) and from an *In Vitro* Transcription and Translation (IVTT) kit. In Figure 10 the DNA binding activities of the HiNF-P point mutations are presented. Panel A indicates an interaction of nuclear extracted wild type and mutant HiNF-P, with 32 P- γ -ATP labeled histone H4/n probe. Mutants with an observed decrease in binding activity are Y381A, Y388A, and S398A/T402A. Mutants with an observed increased binding activity are Y396A and S398A. One mutant, Y381A, displayed no specific band. To ensure that the mutations

truly had no DNA binding activity, films were exposed for extended periods of time (*i.e.* several over-night exposures). Even after the prolonged exposures, no specific band was detected (data not shown). This result indicates that the mutant has no binding activity. In Figure 10 Panel B, the expression of each mutant protein shown. These data suggest that the mutation is not lethal, and that the protein is expressed at similar levels as the wild type so the DNA binding activity can also be compared to wild type DNA binding.

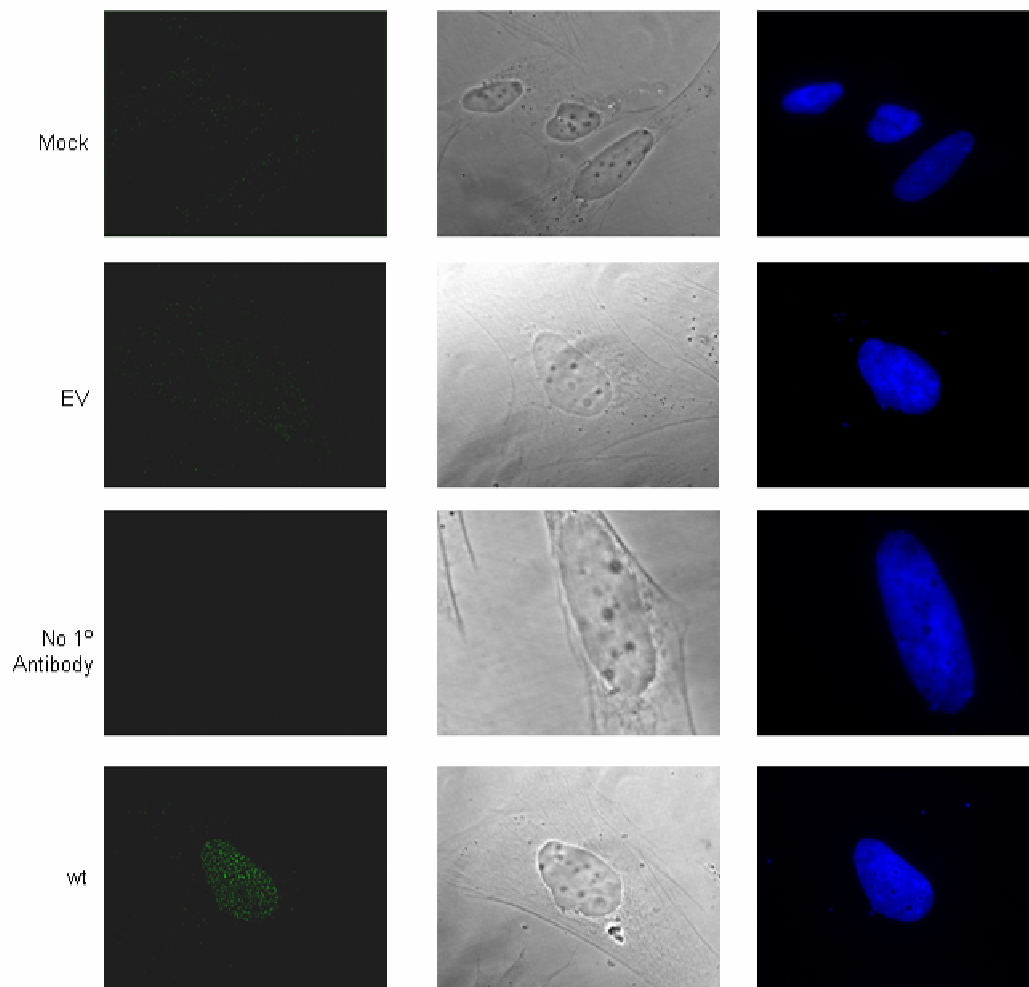


Figure 9a. SaOS immunofluorescence. Wild type HiNF-P shows a nuclear subcellular localization, and all mutations demonstrate that the nuclear localization signal is unaffected. Phase: 200ms; DAPI stain (blue) for DNA 50ms; FITC (green) for HiNF-P 500ms. Panel a presents three negative controls, and wild type. Panels b and c present the experimental mutants. Note: N-term's subcellular localization was determined to be nuclear by previous work (not shown).

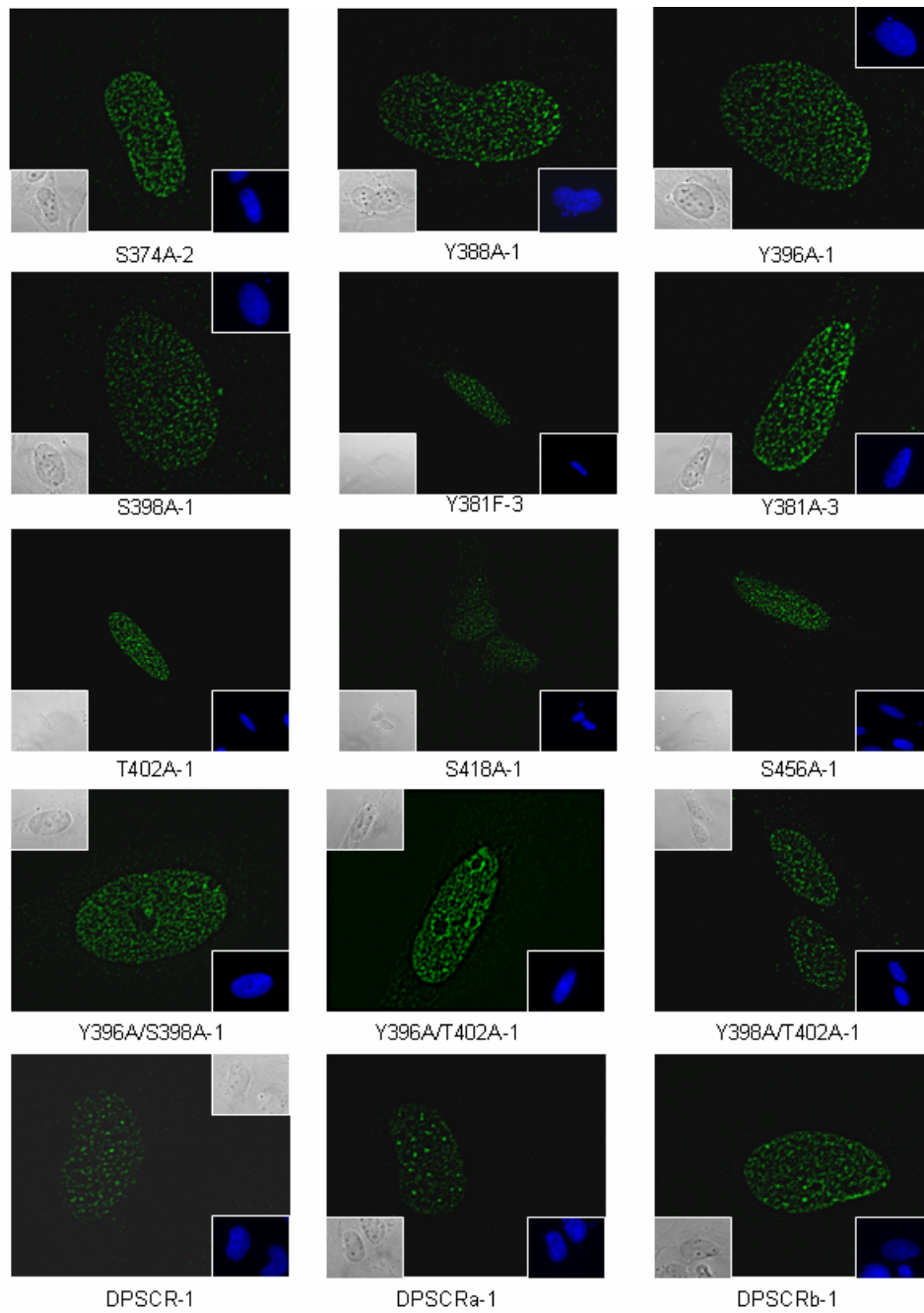


Figure 9b. Immunofluorescence continued.

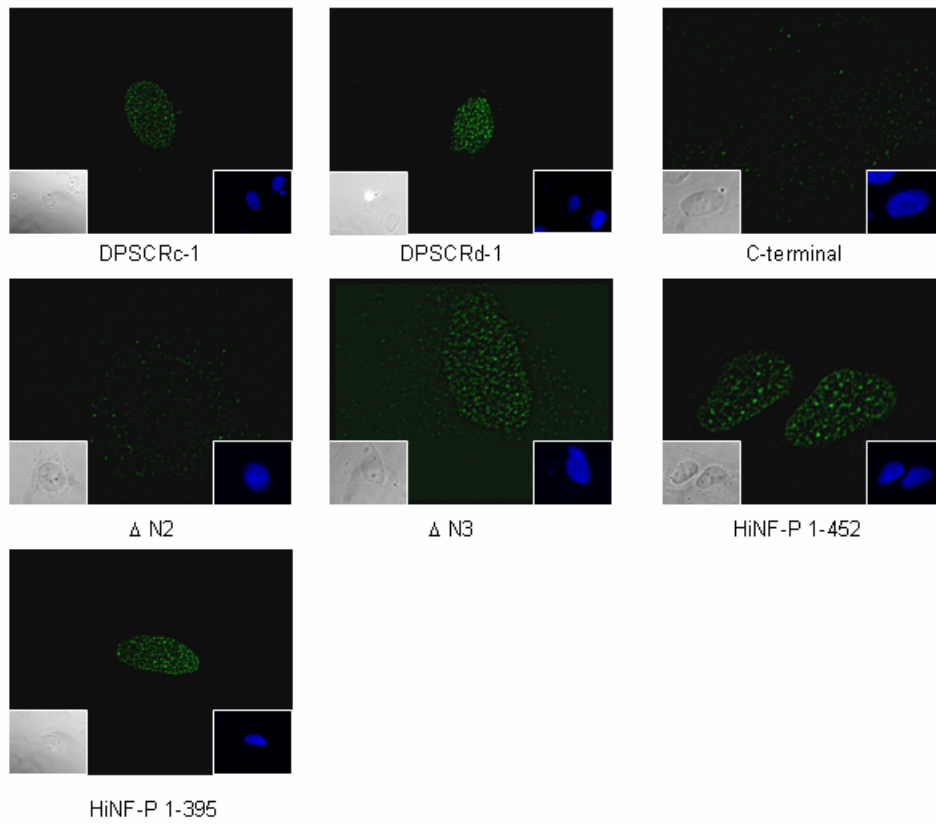


Figure 9c. Immunofluorescence continued.

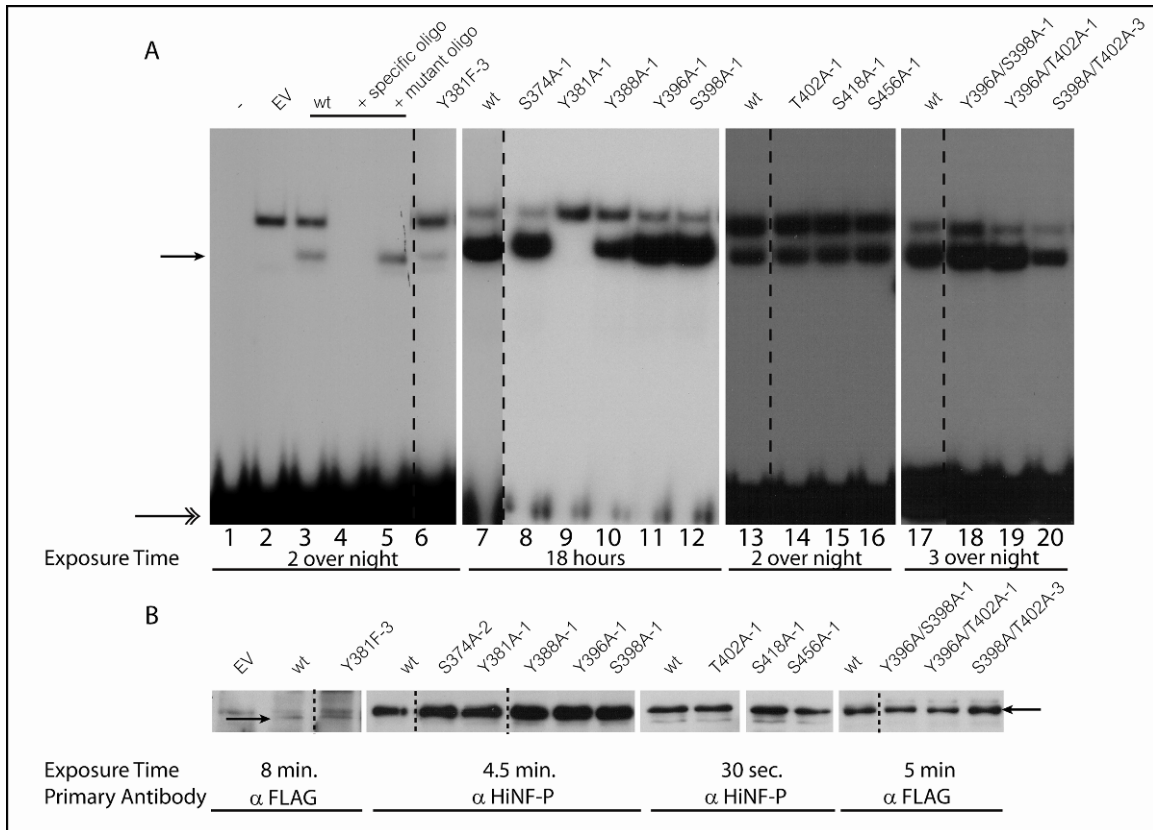


Figure 10. DNA binding activity of mutant HiNF-P as determined by EMSA using HeLa nuclear extracts. (A) Panel A shows two bands, with the specific band indicated by the arrow. The figure is arranged in a way that removes lanes which do not pertain to this report. In order to rank the DNA binding ability of each mutant, each band was compared to the wild type band run from the same experiment. The wild type bands (lanes 3, 7, 13, 17) correspond to the samples that follow immediately to their right until the next wild type band. Free probe is indicated by the double headed arrow. (B) Panel B shows a Western blot, demonstrating that the mutant proteins are being expressed at the expected size, and at similar levels to wild type.

The DNA binding ability of the HiNF-P deletion mutations is shown in Figure 11. The EMSAs in Panel A show increased binding in HiNF-P 1-452, and HiNF-P 1-395. A complete lack of DNA binding ability is observed for the HiNF-P 1-372 (N-term), HiNF-P 373-517 (C-term), HiNF-P 230-517 (Δ N2), HiNF-P 312-517 (Δ N3), Δ PSCR, Δ PSCRa, and Δ PSCRb deletions. All other mutants have similar binding ability as wild type HiNF-P. Protein expression levels were also checked by Western blot, and the results are shown in Panel B. Increased HiNF-P expression was observed for HiNF-P 1-395,

Δ PSCRd, HiNF-P 312-517 (Δ N3), HiNF-P 1-452, and the HiNF-P 1-372 (N-term) deletions. Decreased expression was noticed for Δ PSCR, while the HiNF-P 373-517 (C-term) had no expression at all, which could be caused by a decrease of the protein half life. Future experiments should assay the half life of each mutant protein to determine if it is different from the wild type.

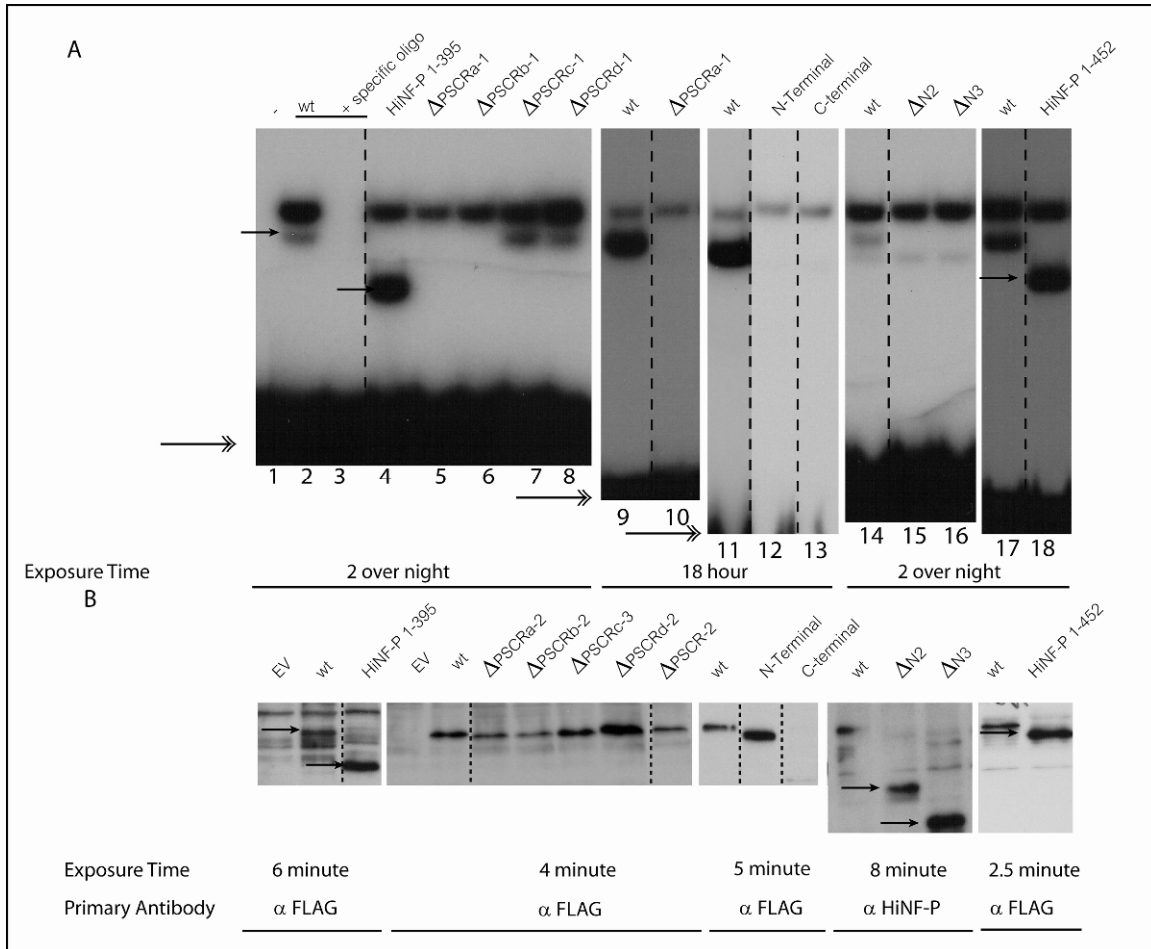


Figure 11. DNA binding activity of HiNF-P deletion mutants as determined by EMSA using HeLa nuclear extracts. (A) Panel A shows two bands, with the HiNF-P specific bands indicated by the single arrowhead arrow on the far left. Lower arrows also point out the specific bands that run faster in the gel because of the truncated protein. The figure is arranged in a way that removes lanes which do not pertain to this report. In order to rank the DNA binding ability of each mutant, each band was compared to the wild type band run from the same experiment. The wild type bands (lanes 2, 9, 11, 14, 17) are used to compare the samples that follow immediately to their right until the next wild type band. Free probe is indicated by the double arrow head. (B) Panel B shows a Western blot, demonstrating that the mutant proteins are being expressed correctly with the expected size, and at similar levels to wild type.

Mutant HiNF-P created by using an IVTT kit was also assayed for DNA binding activity. By synthesizing the protein *in vitro* HiNF-P was assayed without the effects of post translational modifications or interacting proteins. Any effect observed was due solely to the presence of HiNF-P. Figure 12 displays these results. In Panel A, S456A was observed to have decreased binding, while T402A had next to no activity at all, and Y381A did not display any binding activity. An increase in DNA binding ability was observed in S418A, Y396A, and S398A. The Western blot in Panel B shows that all of HiNF-P mutants are expressing.

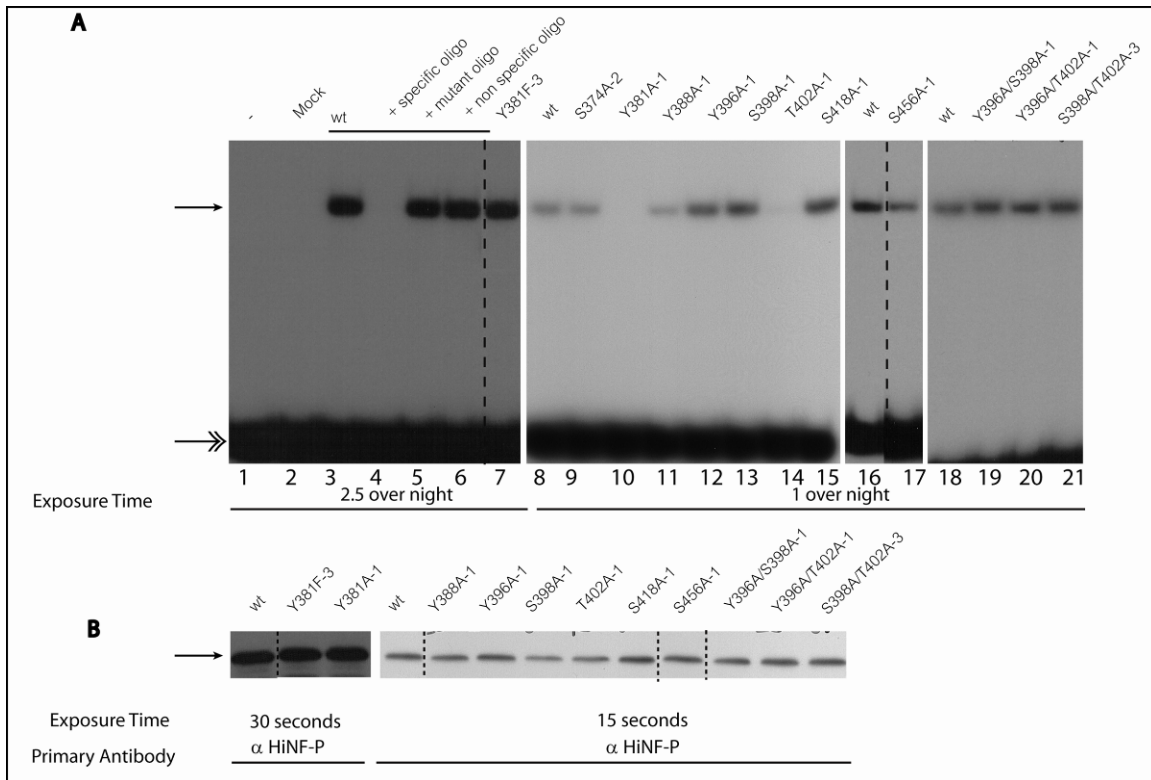


Figure 12. DNA binding activity of IVTT produced mutant HiNF-P as determined by EMSA. (A) Panel A displays the EMSAs, and the HiNF-P specific band is marked by the single arrowhead. The figure is arranged in a way that removes lanes which do not pertain to this report. In order to rank the DNA binding ability of each mutant, each band was compared to the wild type band produced from the same experiment. The wild type bands (lanes 3, 8, 16, 18) are used to compare against the samples that follow immediately to their right until the next wild type band. Free probe is indicated by the double arrow head. (B) Panel B shows a Western blot, demonstrating that the IVTT produced mutant proteins are being expressed correctly.

The deletion mutants produced by IVTT were also assayed in a similar manner (Figure 13). Panel A shows a decrease in HiNF-P 1-395, and HiNF-P 1-452. The HiNF-P 1-372 (N-term), HiNF-P 373-517 (C-term), HiNF-P 230-517 (Δ N2), HiNF-P 312-517 (Δ N3), Δ PSCR, Δ PSCRa, and Δ PSCRb mutations were observed to have no DNA binding activity. In Panel B expression was checked by Western blot. In lane 3 of Panel B an arrow indicates the specific band of HiNF-P 1-395, which is hiding close to the non specific band (identified in the mock lane, and present in the wt lane) mimicking a doublet. All mutant proteins were shown to be expressing, except HiNF-P 373-517 (C-term).

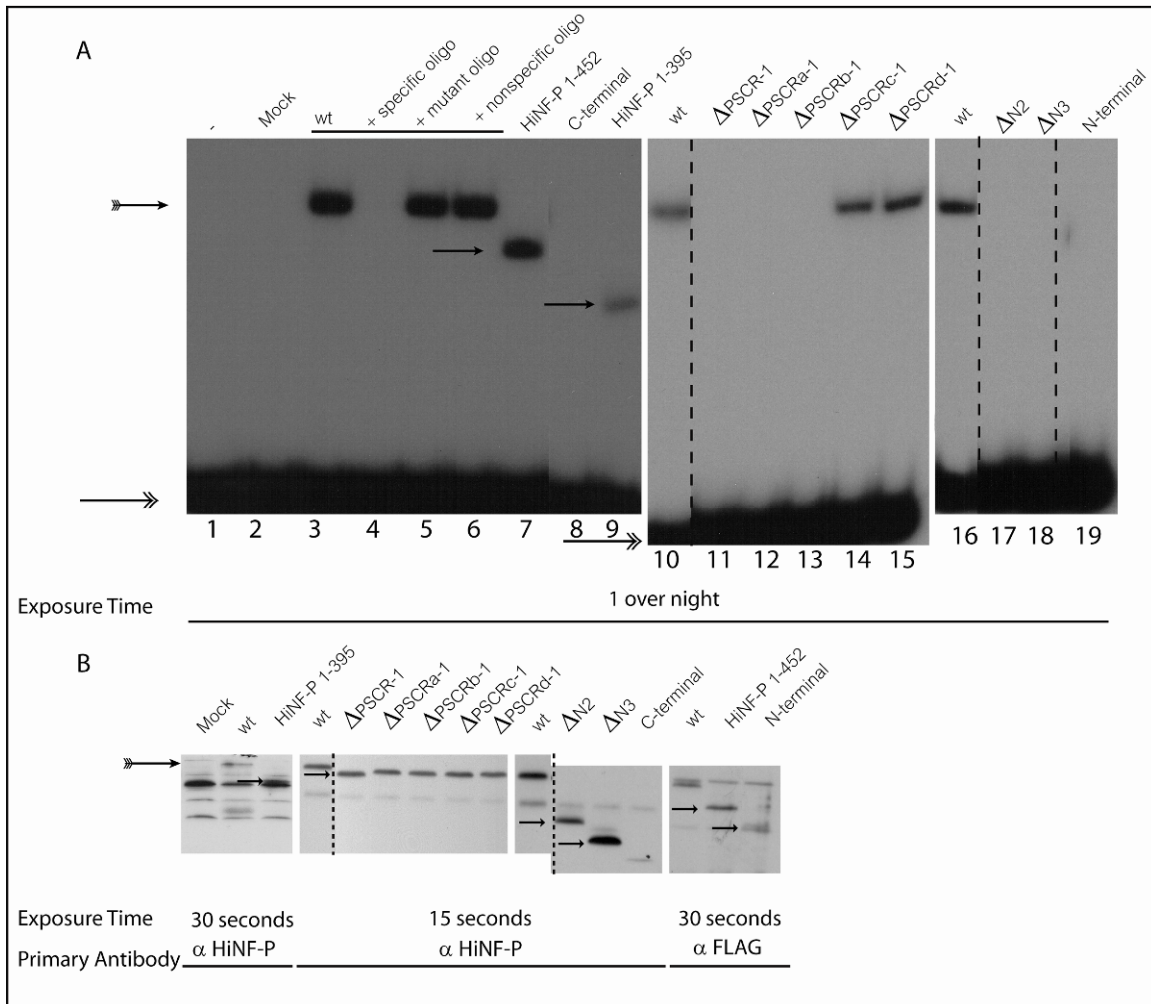


Figure 13. DNA binding activity of IVTT produced HiNF-P deletion mutants as determined by EMSA. (A) Panel A displays the wild type HiNF-P specific band with a feathered arrow, and solid arrows indicate mutant HiNF-P specific bands that migrate faster in the gel because of the deletion. The figure is arranged in a way that removes lanes which do not pertain to this report. In order to rank the DNA binding ability of each mutant, each band was compared to the wild type band run from the same experiment. The wild type bands (lanes 3, 10, 16) are used to compare the samples that follow immediately to their right until the next wild type band. Free probe is shown with a double headed arrow. (B) Panel B shows a Western blot, demonstrating that the IVTT produced mutant proteins are being expressed correctly. A feathered arrow points out the wild type band, and a black arrow points out the specific band of deletion mutants that migrate lower in the gel.

In addition to assaying DNA binding activity, this report also addressed the functional activity of mutant HiNF-P by assaying the effects of the HiNF-P protein on the expression on a multimerized site II promoter driving a luciferase reporter. Figure 14 shows a dose curve in response to increasing amounts of wild type or mutant HiNF-P, as

measured by the luciferase assay. Figure 15 shows the specificity of the reaction by assaying increasing amounts of mutant HiNF-P with a luciferase construct that has Site II (HiNF-P binding domain) mutated. The dosage in both experiments was confirmed by Western blot shown in Figure 16. All but one lane fits the trend of increasing HiNF-P expression. The abnormal lane, Δ PSCRb-1, has lower than expected luciferase activity at the 25 ng level. Figure 16 shows that corresponding expression levels are less than all of the other 25 ng conditions. This low expression, coupled with low luciferase activity suggests an error in the transfection, and that the actual value would be slightly higher.

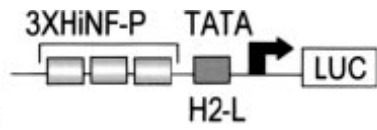
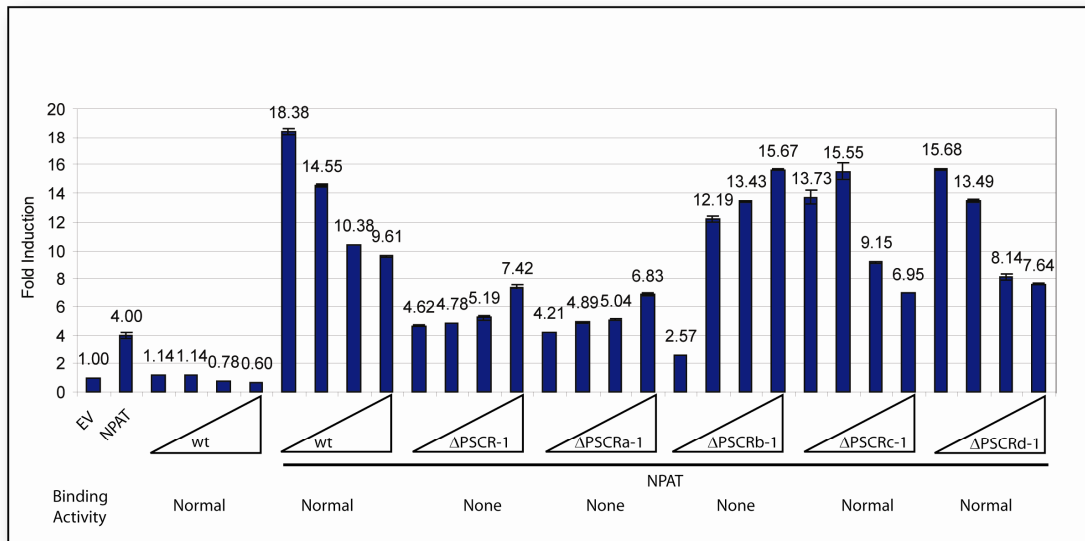
AFrom Mitra *et al.* (2003)**B**

Figure 14. Luciferase activity in response to increasing doses of HiNF-P. (A) Figure of the reporter complex used in the assay. Three site II HiNF-P-binding sites are located upstream of a TATA box, driving a luciferase reporter. (B) This experiment is a composite of two experiments carried out strictly under the same conditions. All values were normalized against *renilla* then normalized again with empty vector set as 1. p3X site II HiNF-P H4n/Luc was used as the reporter. Total amount of DNA was kept constant. Bars 3 through 6 do not contain p220^{NPAT} while lanes 2, and 7 - 30 contain 200ng of p220^{NPAT}.

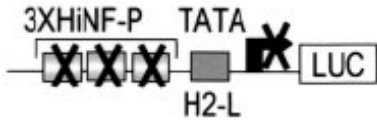
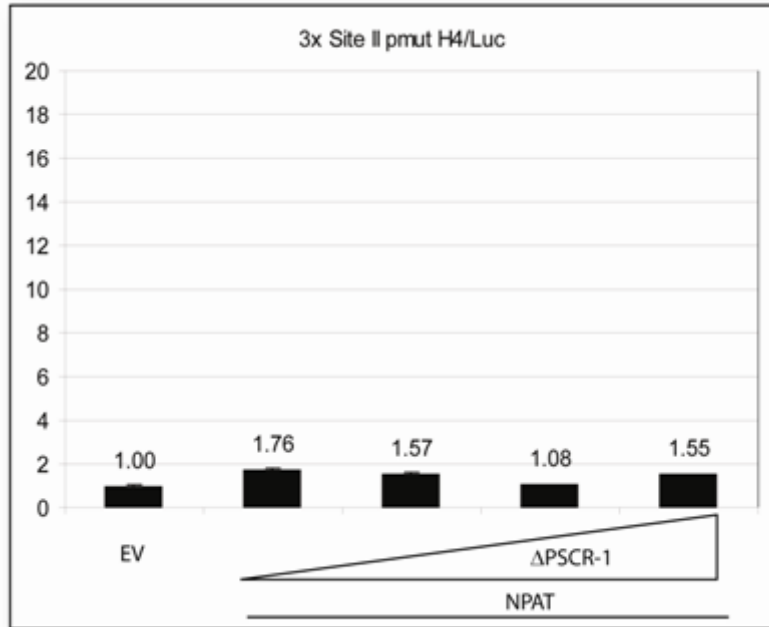
AFrom Mitra *et al.* (2003)**B**

Figure 15. Luciferase activity using the p3X site II HiNF-P mut. H4n/Luc construct. (A) Figure of the reporter complex used in the assay. Three mutated site II HiNF-P-binding sites are located upstream of a TATA box. These multimerized mutated sites do not bind HiNF-P so the luciferase reporter is not activated. (B) Increasing expression of HiNF-P does not bind to mutant site II. This control shows that it is HiNF-P expression that is driving the luciferase reporter, and preventing HiNF-P binding reduces luciferase activity. All values were normalized against *renilla* then normalized again with empty vector set as 1. Total amount of DNA was kept constant.

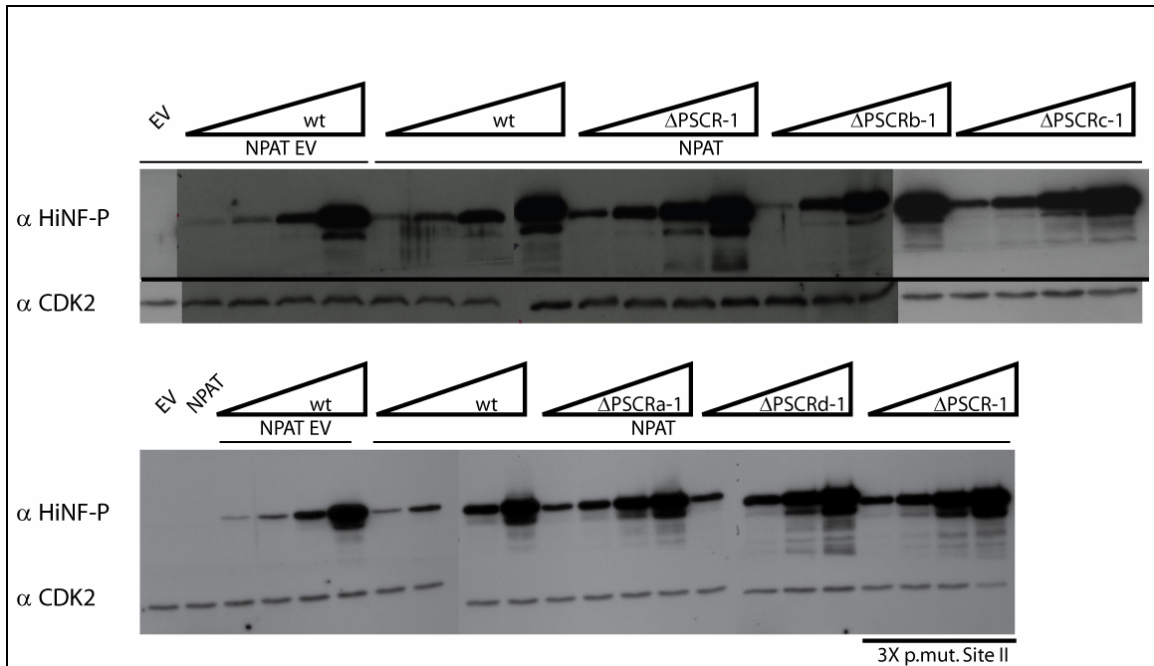


Figure 16. Western blot from luciferase assay lysate shows an increasing amount of HiNF-P expression corresponding with the an increasing amount of transfected plasmid DNA (25ng, 50ng, 100ng, 200ng). The last four lanes of the bottom figure are the samples that were used in the negative control in figure 9. CDK2 was used as a loading control in all samples.

Because of the high levels of overexpressed HiNF-P, the results of a dose curve could be the results of squelching and not a true representation. To account for this the lowest level of mutant HiNF-P construct transfected was plotted separately below in Figure 17. This figure shows that mutants that have no DNA binding activity have 3 to 6 times lower luciferase activity than those which are able to bind DNA.

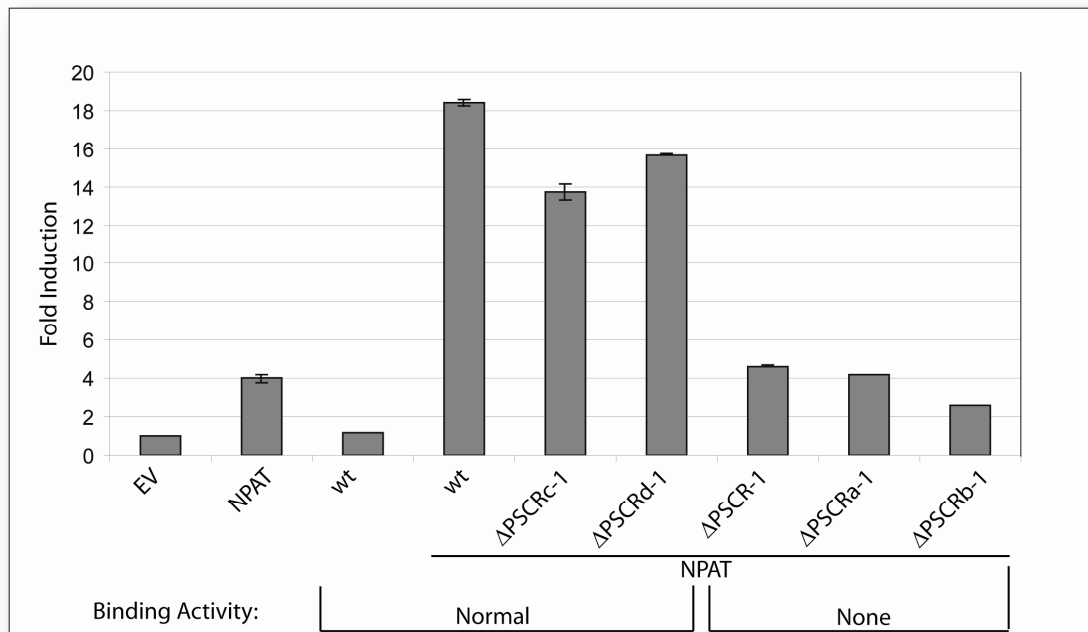


Figure 17. Luciferase activity of the lowest range of transfected HiNF-P constructs suggests that mutants that can not bind DNA (observed by EMSA) have lower luciferase activity than mutants that do bind DNA. p3X site II HiNF-P WT H4n/Luc was used as a reporter and all values were normalized against *renilla* then normalized again with empty vector set as 1. Total amount of DNA was kept constant.

Discussion

To investigate the role the HiNF-P specific conserved region (PSCR) plays in the biological activity of HiNF-P, an extensive mutagenesis project was carried out. Point, double, and deletion mutations were generated and assayed to investigate their DNA binding activity and their ability to activate the histone H4/n promoter. All point mutations were within the defined regions of the PSCR, but two additional point mutants were selected based on their proximity to an acidic region (E339 to E344). Because the PSCR has such a conserved amino acid sequence (Figure 6), it was hypothesized that its function is crucial to HiNF-P. The results presented in this report suggest that the PSCR plays an essential role in DNA binding, and more specifically that a span of the first twenty amino acids of the PSCR (S374- L393) are essential.

Table 3, below, gives a summary of all 23 mutant proteins that were analyzed in this report in regards to DNA binding and protein expression levels. Throughout the duration of this report, successful expression of HiNF-P 373-517 (C-term) was never achieved, which is consistent with previous work conducted in the lab (R. Medina, P. Mitra, personal communication). It is possible that HiNF-P 373-517 (C-term) is not stable enough on its own. This lack of stability would explain the absence of signal in both the immunofluorescence microscopy and in western blots, and in both EMSAs because the protein was not being expressed.

The immunofluorescence data in Figure 9 demonstrate that most mutations did not affect the nuclear localization signal. While S398A and HiNF-P 312-517 (Δ N3) had a higher FITC signal (stain for HiNF-P protein) compared to WT samples, it is possible that overexpressed HiNF-P is being sent into the cytoplasm. The bulk of the immunofluorescence data suggest that the nuclear localization signal is not located within the PSCR.

An interesting finding in this project was the difference in the DNA binding ability of some HiNF-P mutants when overexpressed in cells and assayed in nuclear extracts compared to IVTT produced proteins. In mutants HiNF-P 1-395, HiNF-P 1-452, and HiNF-P T402A there was a decrease in binding activity when the protein was synthesized *in vitro* compared to when it was overexpressed *in vivo*. The most pronounced effect was observed for the HiNF-P mutants 1-395 and T402A. Similar results were observed in HiNF-P S418A, but this mutant had increased binding activity when synthesized *in vitro*. These observations suggest that these specific residues, or amino acids encompassed by the deletion, undergo posttranslational modifications which are not available in the *in vitro* system. Another interesting possibility, that applies to *in vivo* and *in vitro* synthesized protein, is that the mutations are changing HiNF-P protein structure, and therefore its ability to bind DNA is compromised.

HiNF-P Mutant (FLAG)	Sub-cellular Localization	Average Expression	DNA Binding Activity NUC	DNA Binding Activity NTT
Wild Type HiNF-P	Nuclear	3	3	3
S374A	Nuclear	3	3	3
Y381A	Nuclear	3	0	0
Y381F	Nuclear	3	2	3
T402A	Nuclear	3	2.5	.5
S418A	Nuclear	3.5	2	4
S456A	Nuclear	3.5	3.5	2
Y388A	Nuclear	3	3	3
Y396A	Nuclear	4	5	5
S398A	Nuclear (some cytoplasmic)	3.5	4	5
Y396A/S398A	Nuclear	3	3	3
Y396A/T402A	Nuclear	3	3	3
S398A/T402A	Nuclear	3.5	2.5	3
HiNF-P 1-372 (N-term)	Nuclear *	4	0	0
HiNF-P 373-517 (C-term)	No Signal	0	0	0
HiNF-P 230-517 (Δ N2)	Nuclear	3	0	0
HiNF-P 312-517 (Δ N3)	Nuclear (some cytoplasmic)	5	0	0
HiNF-P 1-452	Nuclear	5	4	2
Δ PSCR [Δ 374-407]	Nuclear	1.5	0	0
Δ PSCRa [Δ 374-382]	Nuclear	3	0	0
Δ PSCRb [Δ 383-393]	Nuclear	3	0	0
Δ PSCRc [Δ 394-400]	Nuclear	3	3	3
Δ PSCRd [Δ 401-407]	Nuclear	4	3	3
HiNF-P 1-395	Nuclear	5	5	1

Key

Table 3. Interaction of HiNF-P mutants based on Western blot and EMSA data. * Indicates that this data was observed in previous work (not shown).

HiNF-P mutant Y381A stood out as the only tyrosine mutant that had no binding activity when the tyrosine (Tyr) was mutated to alanine. Because of this, Y381 was selected to be mutated to phenylalanine (Phe), and assayed with the rest of the mutants.

The Phe substitution created a functional mutant that mimics the bulky structure of the original residue, causing fewer structural deviations from wild type HiNF-P. This also allowed a differentiation to be made between a structural phenomenon and a phosphorylation modification, because the only difference between Tyr and Phe is the hydroxyl group in Tyr which is able to be phosphorylated.

We observed that the binding activity of mutants Y381A and Y381F were drastically different. While mutant HiNF-P Y381A shows a complete lack of DNA binding activity, HiNF-P mutant Y381F had near wild type DNA binding. This observation allowed us to rule out the possibility that lack of DNA binding activity of mutant Y381A is due to absence of *in vivo* phosphorylation of Y381, but is most likely due to a structural change produced by this mutation.

We suggest that a structural change also caused increased binding of HiNF-P mutant Y396A. This mutant had identical EMSA results using nuclear extracts and IVTT produced protein, both showing increased DNA binding relative to wild type HiNF-P. Because this effect is observed *in vivo* and *in vitro*, post translational modifications were ruled out. The likely cause is that the mutation results in a structural change, allowing mutant HiNF-P to bind to the site II element in the H4/n promoter with greater affinity.

The luciferase assays demonstrate the ability of a mutant both to bind DNA and to activate transcription. These assays proved to be a large challenge in both implementation and later, interpretation. Figure 14 is a composite of two experiments, strictly carried out under the exact same conditions. It shows that p220^{NPAT} is required for H4/n activation, and together HiNF-P and p220^{NPAT} produce a synergistic effect as shown by Mitra *et al.* (2003).

Though the initial data are in agreement, the trend observed by the luciferase assay when increasing the transfection dose of HiNF-P does not follow the current HiNF-P model. As mentioned in the discussion, HiNF-P does not act alone but acts as a complex with at least one (p220^{NPAT}) if not more co-factors. When expressing excess amounts of HiNF-P well above wild type levels it is possible that the excess HiNF-P may be binding these co-factors, leaving little for the HiNF-P that activates H4/n. This squelching effect would prevent accurate results because with increasing HiNF-P expression a decrease in the amount of co-factors available to bind with potentially biologically active HiNF-P would also follow. We believe this trend observed in Figure 14 to be artificial, and the product of squelching causing non specific luciferase activity.

When working out the conditions to determine how much HiNF-P plasmid to transfect, 25 ng was selected based on its high luciferase activity values. In retrospect, and in light of recent data (not shown), an amount closer to 5 ng would have provided more accurate results since this level of transfection mimics HiNF-P endogenous protein expression levels. Further studies investigating the functional activity of HiNF-P should use this lower dose. Because of the concern that increasing amounts of HiNF-P are causing squelching, analyzing only the lanes transfected with 25 ng (Figure 17) allows for interpretation that follows the EMSA data. Figure 17 illustrates that both binding and non-binding mutants activate the promoter less than wild type and p220^{NPAT} together. More importantly, Figure 17 shows that mutants unable to bind DNA have a 3-6 fold decrease in luciferase activity compared to those that do bind DNA. These results suggest that the PSCR is essential for DNA binding.

Previous work has shown that p220^{NPAT} interacts with the C-terminus of HiNF-P between amino acids 373 and 517 (Miele, *et al.*, 2005). This region spans the PSCR, but also encompasses many other residues. It is possible that some mutants affect NPAT binding, and consequently affect HiNF-P's ability to bind DNA and activate transcription. Future studies should define the NPAT binding site(s) on HiNF-P to rule out disrupting the interaction of HiNF-P and p220^{NPAT}.

The HiNF-P Specific Conserved Region (PSCR) shown in Figure 5 contains a highly conserved amino acid sequence, that likely has a vital role in HiNF-P function. The results of the DNA binding assay suggest that residues in the first twenty amino acids are important in DNA binding. Both *in vivo* (Figure 11) and *in vitro* (Figure 13) EMSAs show that the deletion of the entire Δ PSCR, Δ PSCRa, or Δ PSCRb cause a loss of DNA binding activity. This is further supported by Figure 17 where a substantial decrease in luciferase activity is observed for the same mutants, when compared to wild type HiNF-P. To see what individual residues participate in DNA binding, future research should make point mutants of the twenty amino acids in PSCRa, and PSCRb. This will allow more specific identification of the amino acids that bind and activate H4/n.

The HiNF-P specific conserved region is an area of much interest, because of the high degree of sequence homology throughout many species. In this MQP study, regions of the PSCR were mutated to evaluate the HiNF-P's ability to bind DNA. Experimental observations were made exploring the DNA binding and functional changes induced by the mutations. The mutations caused changes in HiNF-P's ability to bind to DNA and activate histone H4/n promoter. The data in this report suggest that the first twenty amino acids of the PSCR are essential for DNA binding.

References

- Abbott, J., Marzluff, W. F., Gall, J. G. 1999. **The Stem-Loop Binding Protein (SLBP1) Is Present in Coiled Bodies of the Xenopus Germinal Vesicle.** *Mol. Biol. Cell* 10:487-499.
- Alberts, B., Johnson, A., Lewis, J., Raff, M., Roberts, K., Walter, P., (2002). *Molecular Biology of the Cell*. 4th ed. New York, NY: Garland Science.
- Braastad, C. D., Hovhannisyanyan, H., van Wijnen, A. J., Stein, J. L., Stein, G. S. 2004. **Functional characterization of a human histone gene cluster duplication.** *Gene* 342:35-40.
- Frey, M. R., and Matera, G., 1995. **Coiled bodies contain U7 small nuclear RNA and associate with specific DNA sequences in interphase human cells.** *PNAS* 92: 5915–5919.
- Gall, J. G., Bellini, M., Wu, Z., Murphy, C. 1999. **Assembly of the Nuclear Transcription and Processing Machinery: Cajal Bodies (Coiled Bodies) and Transcriptosomes.** *Mol. Biol. Cell* 10: 4385-4402.
- Harris, M. E., Bohni, R., Schneiderman, M. H., Ramamurthy, L., Schumperli, D., Marzluff, W. F. 1991. **Regulation of histone mRNA in the unperturbed cell cycle: evidence suggesting control at two posttranscriptional steps.** *Mol. Cell. Biol.* 11: 2416-2424.
- Imai, T., Yamauchi, M., Seki, N., Sugawara, T., Saito, T., Matsuda, Y., Ito, H., Nagase, T., Nomura, N., Hori, T. 1996. **Identification and characterization of a new gene physically linked to the ATM gene.** *Genome Res.* 6: 439-447.
- Ma, T., Van T., Brian A., Wei, Y., Garrett, M. D., Nelson, D., Adams, P. D., Wang, J., Qin, J., Chow, L. T., Harper, J. W. 2000. **Cell cycle-regulated phosphorylation of p220NPAT by cyclin E/Cdk2 in Cajal bodies promotes histone gene transcription.** *Genes Dev.* 14: 2298-2313.
- Meeks-Wagner, D., and Hartwell, L. H. 1986. **Normal stoichiometry of histone dimer sets is necessary for high fidelity of mitotic chromosome transmission.** *Cell.* 44:43-52.
- Miele, A., Braastad, C. D., Holmes, W. F., Mitra, P., Medina, R., Xie, R., Zaidi, S. K., Ye, X., Wei, Y., Harper, J. W., van Wijnen, A. J., Stein, J. L., Stein, G. S. 2005. **HiNF-P Directly Links the Cyclin E/CDK2/p220NPAT Pathway to Histone H4 Gene Regulation at the G1/S Phase Cell Cycle Transition.** *Mol. Cell. Biol.* 25: 6140-6153.
- Mitra, P., Xie, R. L., Medina, R., Hovhannisyanyan, H., Zaidi, S. K., Wei, Y., Harper, J. W., Stein, J. L., van Wijnen, A. J., Stein, G. S. 2003. **Identification of HiNF-P, a key activator of cell cycle controlled histone H4 genes at the onset of S phase.** *Mol. Cell. Biol.* 23:8110-8123.

- Möröy, T., and Geisen, C. 2004. **Cyclin E**. *Int. J. Biochem. Cell Biol.* 36:1424-1439.
- Osley, M. A. 1991. **Regulation of histone synthesis in the cell cycle**. *Annu. Rev. Biochem.* 60:827-861
- Pauli U., Chrysogelos S., Stein G., Stein J., Nick H. 1987. **Protein-DNA interactions in vivo upstream of a cell cycle-regulated human H4 histone gene**. *Science*. Jun 236:1308-1311
- Stein, G. S., van Wijnen, A. J., Stein, J. L., Lian, J. B., Montecino, M., Zaidi, S. K., Braastad, C. 2006. **An Architectural Perspective of Cell-Cycle Control at the G1/S Phase Cell-Cycle Transition**. *J. Cell. Phys.* 209:706-710.
- Stevens, C., La Thangue, N. 2003. **E2F and cell cycle control: a double-edged sword**. *Arch Biochem Biophys.* 2:157-169.
- van Wijnen A. J., Ramsey-Ewing A. L., Bortell R., Owen T. A., Lian J. B., Stein J. L., Stein G. S. 1991. **Transcriptional element H4-site II of cell cycle regulated human H4 histone genes is a multipartite protein/DNA interaction site for factors HiNF-D, HiNF-M, and HiNF-P: involvement of phosphorylation**. *J. Cell. Biochem.* 46:174-189.
- van Wijnen, A. J., van den Ent, F., Lian, J., Stein, J., Stein G., 1992. **Overlapping and CpG Methylation-Sensitive Protein-DNA Interactions at the Histone H4 Transcriptional Cell Cycle Domain: Distinctions between Two Human H4 Gene Promoters**. *Mol. Cell. Biol.* 12:3273-3287.
- Wu, R. S., and Bonner, W. M. 1981. **Separation of basal histone synthesis from S-phase histone synthesis in dividing cells**. *Cell.* 27:321-330.
- Zhao, J., Dynlacht, B., Imai, T., Hori, T., Harlow, E. 1998. **Expression of NPAT, a novel substrate of cyclin E-CDK2, promotes S-phase entry**. *Genes Dev.* 12: 456-461.
- Zhao, J., Kennedy, B., Lawrence, B., Barbie, D., Matera, A., Fletcher, J., Harlow, E. (2000) **NPAT links cyclin E-Cdk2 to the regulation of replication-dependent histone gene transcription**. *Genes Dev.* 14: 2283-2297.